

Weak corrections to gluon-induced top-antitop hadro-production

S. Moretti, M.R. Nolten and D.A. Ross

School of Physics & Astronomy, University of Southampton, Southampton SO17 1BJ, UK

Abstract

We calculate purely weak virtual one-loop corrections to the production cross section of top-antitop pairs at the Large Hadron Collider via the gluon-gluon fusion subprocess. We find very small negative corrections to the total cross section, of order -0.6% , but significantly larger effects to the differential one, particularly in the transverse momentum distribution, of order -5% to -10% (in observable regions). In case of parity-conserving spin-asymmetries of the final state, $\alpha_S^2\alpha_W$ corrections are typically of a few negative percent, with the exception of positive and negative peaks at $+12\%$ and -5% , respectively (near where the tree-level predictions change sign), while those arising in parity-violating asymmetries (which are identically zero in QCD) are typically at a level of a few permille.

1 Introduction

Top quark physics may well be the only context where both accurate Standard Model (SM) tests and searches for new physics Beyond the Standard Model (BSM) will be carried out at the Large Hadron Collider (LHC). If no BSM physics exists at the TeV scale or the typical mass scale of new particles is (just) above the energy reach of the machine, one may well conceive that most of the experimental and theoretical efforts will concentrate in establishing the true nature of the top quark, which in turn will also enable one to constrain possible manifestations of new physics. While top quarks have been discovered and studied at the Tevatron, the reduced number of events available there will only allow one for a percent level determination of the top mass (currently, $m_t = 172.7 \pm 2.9$ GeV). This precision will be improved by over a factor of two at the CERN machine. Here, one will also be able to measure the top-quark width and quantum numbers (i.e., the electric charge and isospin, accessible through its Electro-Weak (EW) couplings). While there is certainly scope to investigate the EW couplings of top-quarks by resorting to events with radiated photons and Z bosons [1], the $V - A$ structure (or otherwise) of the charged decay current can already be probed directly in $t\bar{t}$ events, if one recalls that the top-(anti)quark decays into a bottom-(anti)quark and a W boson rather than hadronising. Finally, for the

same reason, the top-(anti)quark transmits its spin properties to the decay products rather efficiently, so that the latter can be explored in suitable experimental observables [2, 3, 4].

Clearly, in order to perform all the relevant measurements in $t\bar{t}$ events, any source of SM corrections should be well under control. While complete one-loop results exist for QCD [5], similar weak effects have been unavailable until very recently [6, 7]. These last two papers were concerned with purely weak $\alpha_S^2\alpha_W$ effects entering the $q\bar{q} \rightarrow t\bar{t}$ subprocess only. It is the purpose of this paper to complement those studies, by computing the corrections to the $gg \rightarrow t\bar{t}$ channel, which is in fact dominant at the LHC (whereas the quark initiated one is the leading partonic component at the Tevatron). Early, though incomplete results, for $\alpha_S^2\alpha_W$ corrections to top-antitop hadro-production can be found in Ref. [8] for both gg and $q\bar{q}$ initiated subprocesses. Concerning the $gg \rightarrow t\bar{t}$ case, unlike Ref. [8], notice that we have also included here the one-loop triangle contributions for $gg \rightarrow Z^* \rightarrow t\bar{t}$, which are in fact non-zero for off-shell Z bosons. (Recall that the Landau-Yang’s theorem [9] is only valid for on-shell Z bosons and we have explicitly verified this to be the case in our calculation if we take the appropriate limit.) We have also updated the analyses of [8] to the most recent top and Higgs mass values as well as Parton Distribution Functions (PDFs).

The paper is organised as follows. The next section illustrates the importance that EW effects should have at TeV energy scales. Sections 3 and 4 will be devoted to describe our computation and present the numerical results, respectively. The last section contains our conclusions.

2 EW effects at TeV scale energies

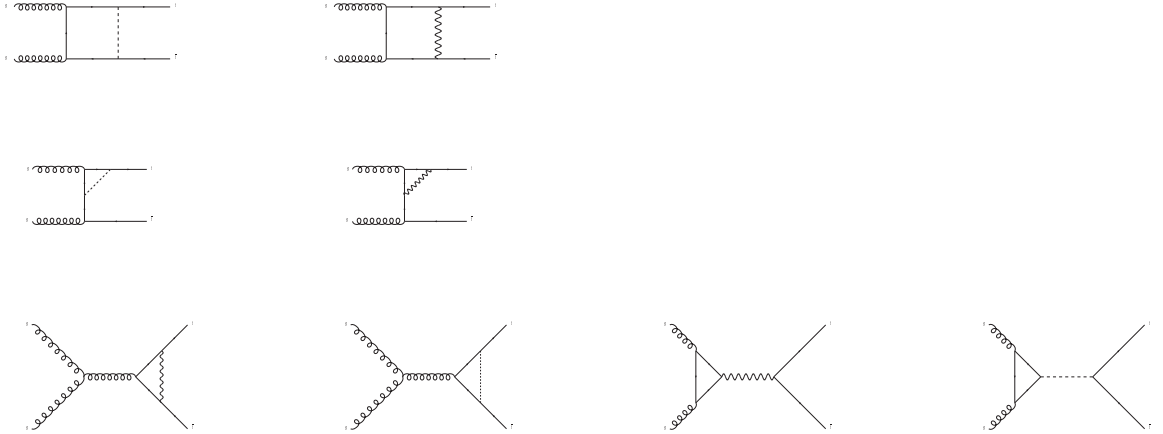
The purely weak (W) component of Next-to-Leading Order (NLO) EW effects produces corrections of the type $\alpha_W \log^2(\mu^2/M_W^2)$, where $\alpha_W \equiv \alpha_{\text{EM}}/\sin^2\theta_W$, with α_{EM} the Electro-Magnetic (EM) coupling constant and θ_W the Weinberg angle. Here, μ represents some typical energy scale affecting the top-antitop process in a given observable, e.g., the transverse momentum of either the top (anti)quark or the top-antitop invariant mass. For large enough μ values, such EW effects may be competitive not only with Next-to-NLO (NNLO) (as $\alpha_W \approx \alpha_S^2$) but also with NLO QCD corrections (e.g., for $\mu = 0.5$ TeV, $\log^2(\mu^2/M_W^2) \approx 10$).

These ‘double logs’ are of Sudakov origin and are due to a lack of cancellation between virtual and real W -emission in higher order contributions. This is in turn a consequence of the violation of the Bloch-Nordsieck theorem in non-Abelian theories [11, 12]. The problem is in principle present also in QCD. In practice, however, it has no observable consequences, because of the final averaging of the colour degrees of freedom of partons, forced by confinement into colourless hadrons. This does not occur in the EW case, where the initial state generally has a non-Abelian charge, as in proton-proton scattering. Besides, these logarithmic corrections are finite (unlike in QCD), since M_W provides a physical cut-off for W -emission. Hence, for typical experimental resolutions, softly and collinearly emitted weak bosons need not be included in the production cross section and one can restrict oneself to the calculation of weak effects originating from virtual corrections only. By doing so, similar

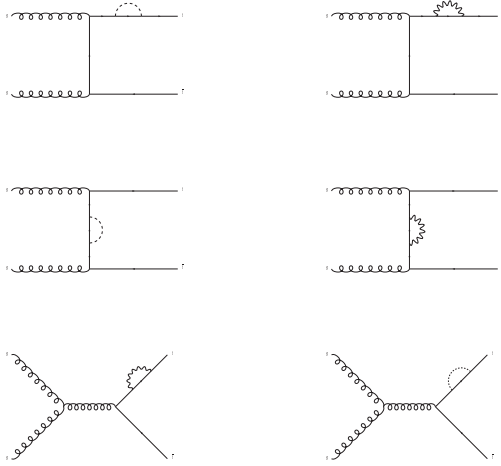
logarithmic effects, $\sim \alpha_W \log^2(\mu^2/M_Z^2)$, are generated also by Z -boson corrections. Finally, in some instances all these purely weak contributions can be isolated in a gauge-invariant manner from EM effects which therefore may not be included in the calculation (as it is the case here). (Besides, EM corrections are not subject to Sudakov enhancement.) In view of all this, it becomes of crucial importance to assess quantitatively such weak corrections affecting, in particular, a key process (for both present and future hadron colliders) such as top-antitop hadro-production.

3 Calculation

It is the aim of our paper to report on the computation of the full one-loop weak effects entering the subprocess $gg \rightarrow t\bar{t}$, through the perturbative order $\alpha_S^2\alpha_W$. We will instead ignore altogether the contributions of tree-level $\alpha_S^2\alpha_W$ terms involving the radiation (bremsstrahlung) of real Z bosons. In the Feynman-'t Hooft gauge¹, the one used for this calculation, neglecting the b -mass, one has to calculate the following one-loop prototype diagrams for $gg \rightarrow t\bar{t}$, ignoring permutations of external gluons:



¹Here, we mean that the numerator of the massive gauge boson propagators is taken to be $-ig_{\mu\nu}$ and Goldstone bosons, with masses equal to their gauge boson counterparts, are included where appropriate.



(In the calculation of all such graphs, we have retained the full spin dependence of the final state particles.)

Given the large number of diagrams involved in the computation, it is of paramount importance to perform careful checks. In this respect, we should mention that our expressions have been calculated independently by at least two of us using FORM [13] and that some results have also been reproduced by another program based on FeynCalc [14]. Upon removing the one-loop triangle contributions for $gg \rightarrow Z^* \rightarrow t\bar{t}$ and for identical choices of Higgs mass, we also reproduce well the results of the first paper in Ref. [8]. (In fact, this triangle contribution is always only marginally relevant.) Finally, we find reasonable agreement with Ref. [4] (see also [15, 16]) in the Sudakov limit, i.e., for large invariant masses and transverse momenta of the final state, provided that the final state particles are fairly central (see later on).

Some of the diagrams contain ultraviolet divergences. In the case of self-energies for massive particles the mass subtraction has been effected on mass-shell so that the masses refer to the physical (pole) masses. The remaining divergences have been subtracted using the ‘modified’ Dimensional Reduction ($\overline{\text{DR}}$) scheme at the scale $\mu = M_Z$. The use of $\overline{\text{DR}}$, as opposed to the more usual ‘modified’ Minimal Subtraction ($\overline{\text{MS}}$) scheme, is forced upon us by the fact that the W and Z bosons contain axial couplings which cannot be consistently treated in ordinary dimensional regularisation. The strong coupling is *not* renormalised by the weak interactions, which means that there are Ward identities which cancel the divergent corrections to the strong coupling. Thus the choice of subtraction scheme has no effect on our final results since the scheme dependence cancels when all graphs are summed over. On the other hand the EM coupling, α_{EM} , has been taken to be $1/128$ in order to

correctly account for the SM running of the electroweak coupling up to the threshold for $t\bar{t}$ production.

For the top mass and width, the latter entering some of the loop diagrams, we have taken $m_t = 175$ GeV and $\Gamma_t = 1.55$ GeV, respectively. (As already intimated, the b -quark was considered massless.) The Z mass used was $M_Z = 91.19$ GeV and was related to the W mass, M_W , via the SM formula $M_W = M_Z \cos \theta_W$, where $\sin^2 \theta_W = 0.232$. (Corresponding widths were $\Gamma_Z = 2.5$ GeV and $\Gamma_W = 2.08$ GeV.) The Higgs boson mass and width were set to 150 GeV and 16 MeV by default, respectively. However, other mass (and consequently width) choices (above the LEP limit of $M_H \gtrsim 115$ GeV) have been investigated (see later on). The PDFs we have used are CTEQ6L1 [17] taken at the factorisation scale $Q = 2m_t$. We have also checked other sets, but found no significant difference in the relative size of our corrections.

4 Numerical results

Our initial findings are presented in Figs. 1–2. Here, we consider both differential spectra of some kinematic observables as well as global asymmetries, the latter plotted, e.g., against the invariant mass of the $t\bar{t}$ pair. Notice that this last quantity can only be defined when both the top and anti-top four-momenta are reconstructed, which happens in the case of fully hadronic and semi-leptonic/hadronic decays², but not for fully leptonic ones (where two neutrinos escape detection).

The definitions of the asymmetries are as follows:

$$\begin{aligned} A_{LL} d\sigma &\equiv d\sigma_{++} - d\sigma_{+-} + d\sigma_{--} - d\sigma_{-+}, \\ A_L d\sigma &\equiv d\sigma_- - d\sigma_+, \\ A_{PV} d\sigma &\equiv d\sigma_{--} - d\sigma_{++}. \end{aligned} \tag{1}$$

For A_L only the polarisation of *either* the t -quark or t -antiquark is assumed to be measured, whereas the other two asymmetries require the determination of the polarisations of *both* the outgoing particles. A_{LL} is parity-conserving while the other two are parity-violating³. Here, the indices $+$ and $-$ refer to the helicities of right (R) and left (L) handed (anti)top quark, respectively. (Other basis choices are also possible, see Ref. [2].)

We find that the overall effect of our $\mathcal{O}(\alpha_S^2 \alpha_W)$ corrections is about -0.6% at the inclusive level (i.e., to the total cross section, as obtained from the integral of any of the curves in Fig. 1). However, for differential cross sections, effects can be of either sign, notably in the (anti)top transverse momentum and top-antitop invariant mass. For an LHC integrated luminosity of 300 fb^{-1} , differential rates of order a few 10^{-5} pb may yield detectable events (after accounting for decay fractions, tagging efficiency and reconstruction performance).

²In the second case one would reconstruct the longitudinal neutrino momentum by equating the transverse one to the missing transverse energy and enforcing the W mass reconstruction.

³See Ref. [2] for a choice of observables correlated to these asymmetries.

In the corresponding observable kinematic range, the maximum correction occurs for the transverse momentum spectrum of the (anti)top at around 1 TeV (in the Sudakov limit), where it reaches almost the -10% level. In the same kinematic regime, the effects are smaller for the invariant mass and pseudorapidity distributions. At small transverse momentum, invariant mass as well as in the very forward/backward direction is where the corrections are positive, with a maximum of $\mathcal{O}(+2\%)$ for the second of these observables.

In the case of the parity-conserving asymmetry, for which the $\mathcal{O}(\alpha_S^2)$ result is non-zero, $\mathcal{O}(\alpha_S^2\alpha_W)$ effects enter significantly (up to the $+12$ and -5% level or so) only near the point where tree-level predictions are zero. Otherwise, they amount to a few negative percent at the most. For the parity-violating asymmetries, the relevant quantity is the actual value of the $\mathcal{O}(\alpha_S^2\alpha_W)$ result, as the $\mathcal{O}(\alpha_S^2)$ term is identically zero. In both cases, the rates are at the permille level (away from the $M_{t\bar{t}} \approx 2m_t$ threshold, where our fixed order results are not fully reliable).

The dependence on the actual value of the Higgs mass is generally negligible at both inclusive as well as differential level, with the possible exception of the pseudorapidity distribution in the very central region, see Fig. 3 (top-left frame), where the absolute size of the $\mathcal{O}(\alpha_S^2\alpha_W)$ corrections is shown for $M_H = 150$ and 200 GeV. In fact, the inclusive correction varies from -2.33 to -2.51 pb, respectively, in comparison to a (Higgs independent) tree-level result of 384 pb. For the other differential spectra studied such effects are rather uniformly spread across the given kinematic range. As for the asymmetries, here the effect of an increased Higgs mass varies significantly with $M_{t\bar{t}}$, yielding differences with respect to the rates obtained with our default Higgs mass value which are not negligible over most of the kinematical intervals considered, see Fig. 3 (top-right and bottom frames).

Before closing, it is of interest to compare our exact $\mathcal{O}(\alpha_S^2\alpha_W)$ results with those of Ref. [4]. Notice that the latter only include the case of opposite helicities⁴ in the final state and are limited to the contribution of non-angular single ($\sim \alpha_W \log(s/M_W^2)$) and double ($\sim \alpha_W \log^2(s/M_W^2)$) logarithms. In performing the comparison between our results and those in Ref. [4] we have removed the EM component from the latter. From Fig. 4, it is clear that for the logarithmic approximation described be valid all Mandelstam variables $\hat{s}, \hat{t}, \hat{u}$ must be very large, condition which is obviously not fulfilled at small/large scattering angles. However, it should be appreciated that the ratio between the full $\mathcal{O}(\alpha_S^2\alpha_W)$ term and the one obtained in NLO Sudakov approximation is a constant to a very good approximation already at moderate energies and for most angles. Thus, in principle, a parameterisation of this constant as a function of the angle should be possible, in view of high statistics Monte Carlo simulations.

⁴The contribution due to identical final state helicities becomes not negligible near the threshold at $M_{t\bar{t}} \approx 2m_t$.

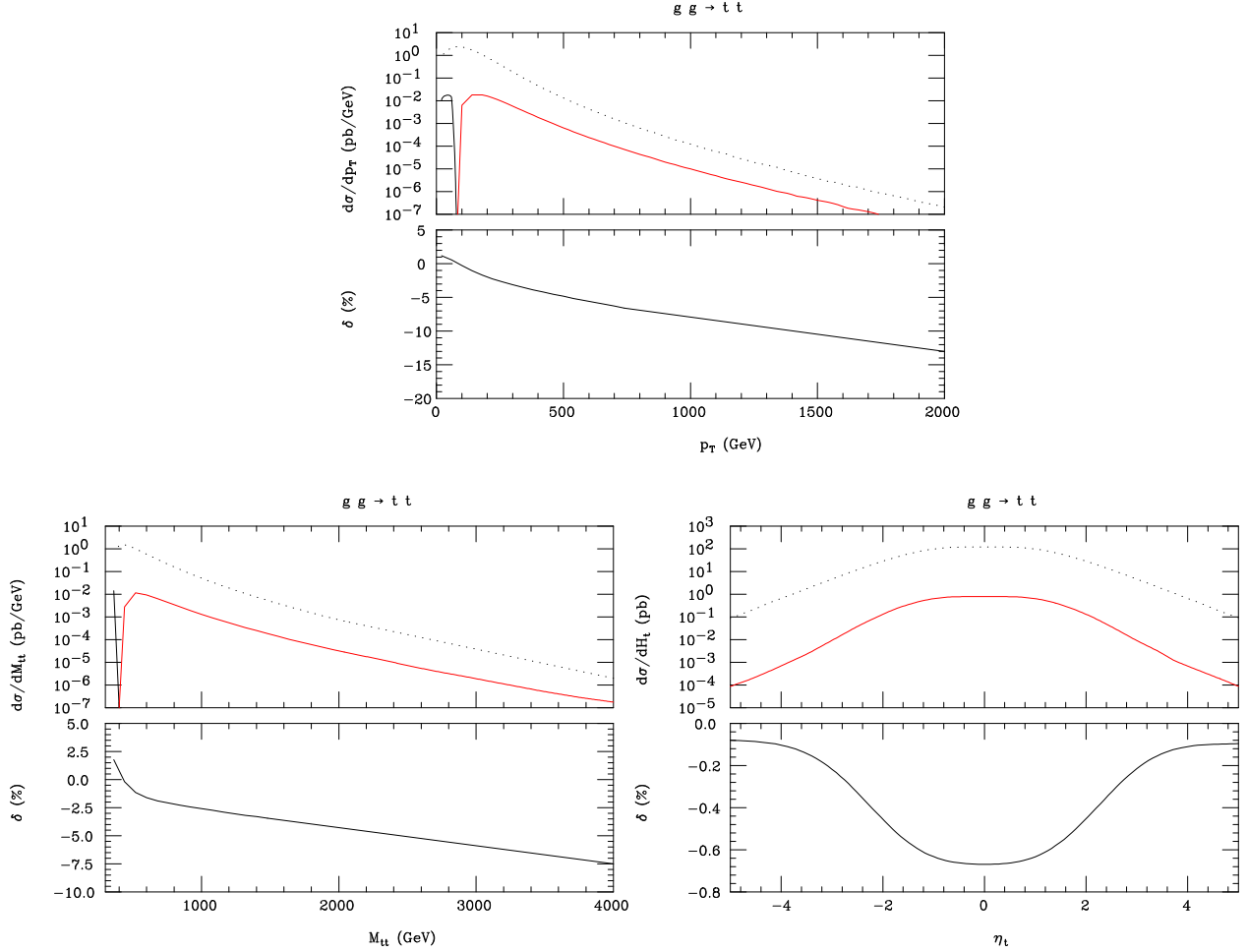


Figure 1: Differential distributions of the subprocess $gg \rightarrow t\bar{t}$ through the $\mathcal{O}(\alpha_s^2)$ (top frames, dotted) and the $\mathcal{O}(\alpha_s^2 \alpha_W)$ (top frames, solid) as well as the percentage of the latter with respect to the former (bottom frames, solid) for the (anti)top transverse momentum p_T , the top-antitop invariant mass $M_{t\bar{t}}$ and the (anti)top pseudorapidity η_t . (Lightly/Red coloured solid tracts in logarithmic scale are intended to be negative.)

5 Conclusions and outlook

For kinematic variables accessible at the LHC, purely weak corrections through one-loop level (without Z bremsstrahlung) to the top-antitop cross section via gluon-gluon fusion are generally small, although – in order to obtain both the appropriate normalisation and shape of the theoretical prediction – they cannot be neglected in the Sudakov regime of some observables. In contrast, in line with the results reported in [18]–[21] for the case of massless quark pair production, such one-loop weak effects are always crucial in massive quark pair production when spin-asymmetries are considered (particularly, parity-violating ones). Ultimately, our results will have to be put together with those from Refs. [6, 7] (which we are in the process of repeating), in order to study the top-antitop cross section

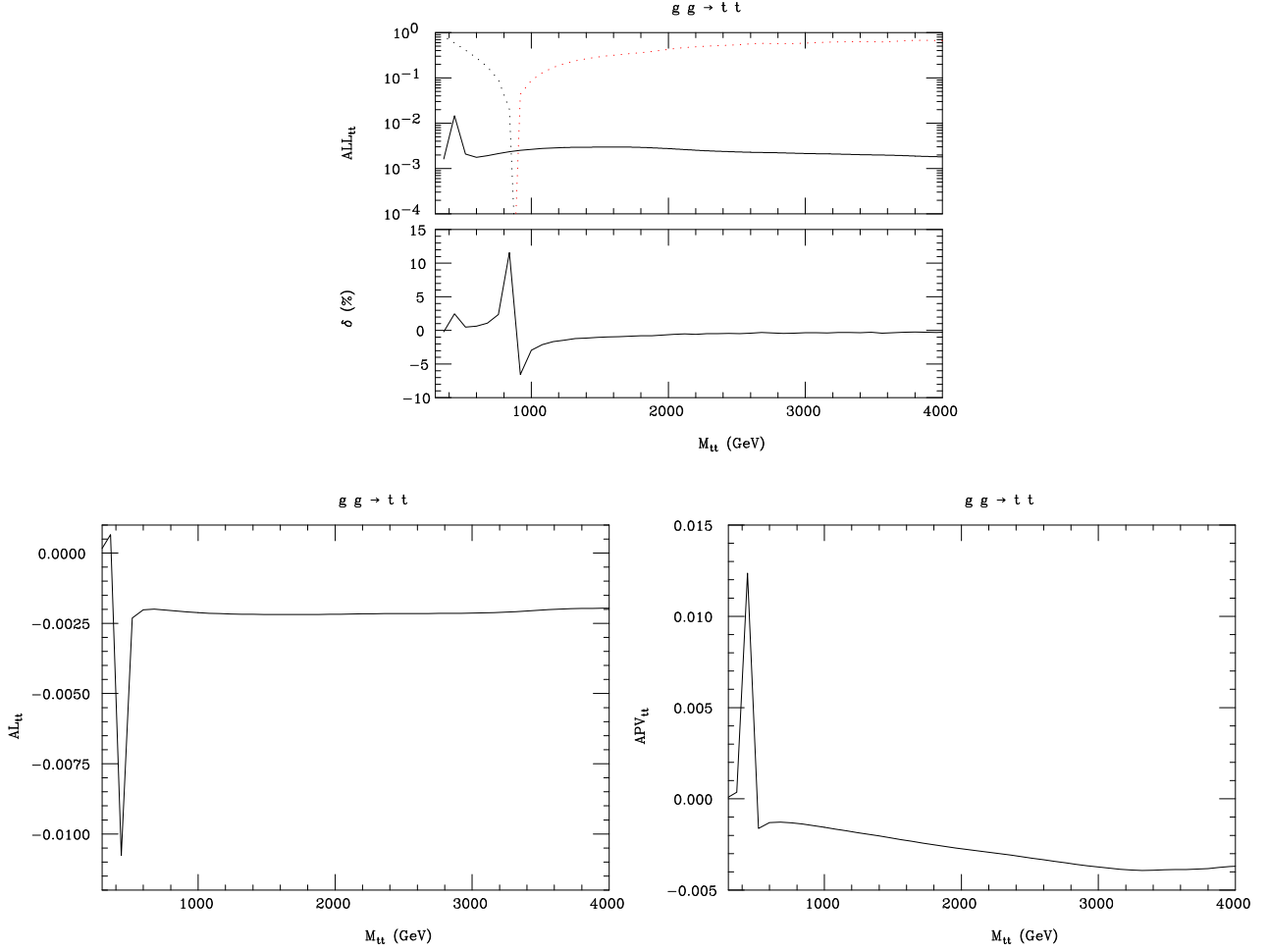


Figure 2: The differential spin asymmetry A_{LL} (as defined in the text) of the subprocess $gg \rightarrow t\bar{t}$ through the $\mathcal{O}(\alpha_s^2)$ (top frame, dotted) and the $\mathcal{O}(\alpha_s^2\alpha_W)$ (top frame, solid). (Note that the LO QCD contribution changes sign at ≈ 900 GeV and is heavily dependent on $M_{t\bar{t}}$ whereas the $\mathcal{O}(\alpha_s^2\alpha_W)$ correction is not.) Just below the top frame we show the percentage correction to the (non-zero) LO QCD asymmetry for A_{LL} due to $\mathcal{O}(\alpha_s^2\alpha_W)$ effects. The lower two frames display the asymmetries A_L and A_{PV} (as defined in the text), which vanish exactly in LO QCD, through the same order. The asymmetries are calculated along the helicity axis as a function of the top-antitop invariant mass $M_{t\bar{t}}$.

at the level of precision required by the LHC experiments. However, particular care should eventually be devoted to the treatment of real Z production and decay in the definition of the inclusive data sample, as this will determine whether (possibly positive) tree-level Z bremsstrahlung effects have to be included in the theoretical predictions through $\mathcal{O}(\alpha_s^2\alpha_W)$, which might counterbalance the negative effects due to the one-loop Z exchange estimated here. Along the same lines, it should be recalled that NNLO terms ought to be investigated too, as it is well known from the Sudakov treatment that they may well be sizable in comparison to the NLO ones (see, e.g., Ref. [22]). Finally, we have verified that the effects

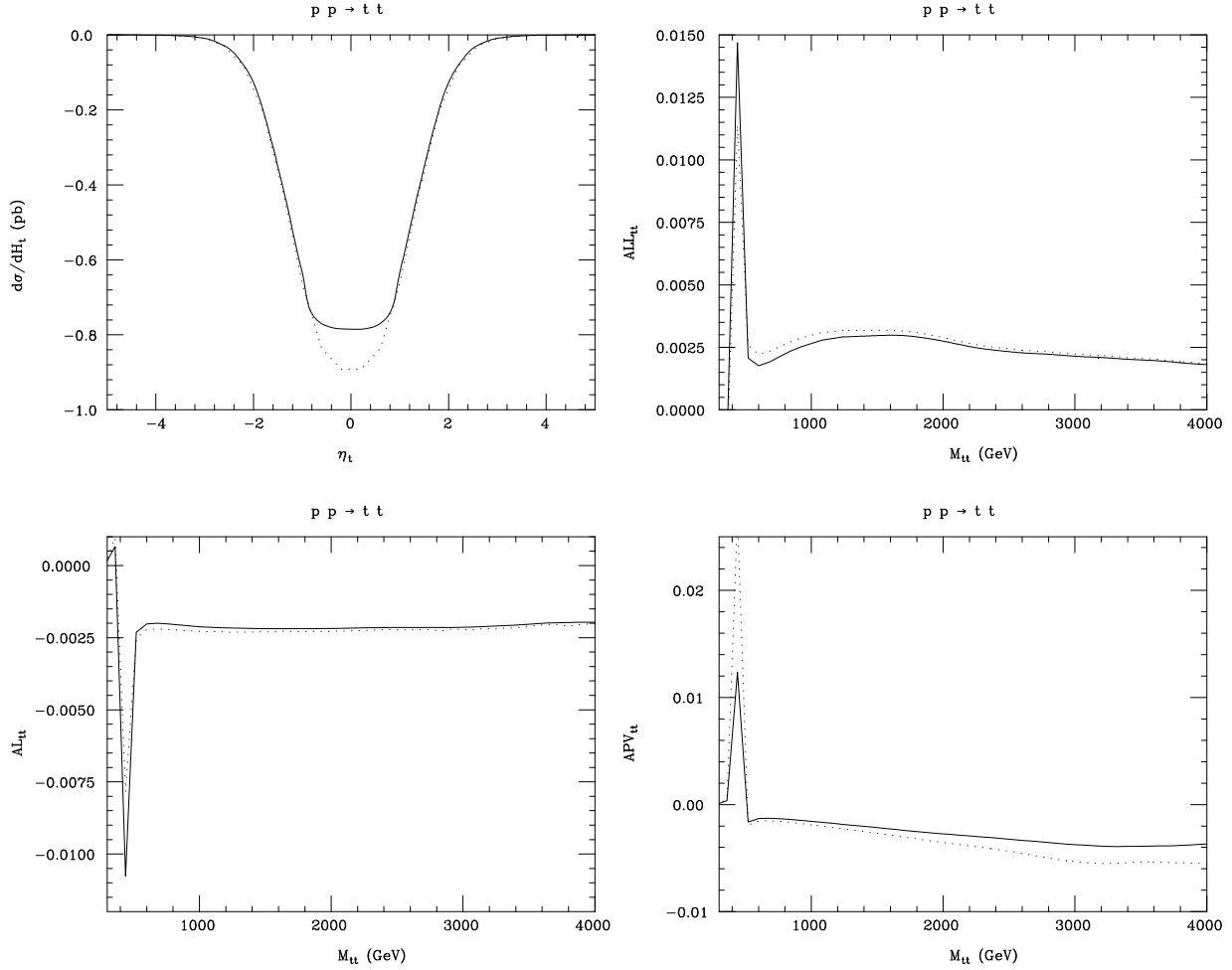


Figure 3: The absolute size of the $\mathcal{O}(\alpha_s^2 \alpha_W)$ corrections to the subprocess $gg \rightarrow t\bar{t}$ for the distribution in (anti)top pseudorapidity η_t (top-left frame) and the differential spin asymmetries (as defined in the text), for $M_H = 150$ GeV (solid) and $M_H = 200$ GeV (dotted). The asymmetries are calculated along the helicity axis as a function of the top-antitop invariant mass $M_{t\bar{t}}$.

studied here for the $gg \rightarrow t\bar{t}$ channel are of no phenomenological relevance at the Tevatron. The experimental impact of $\mathcal{O}(\alpha_s^2 \alpha_W)$ effects will eventually have to be assessed in a proper detector simulation, in presence of top-antitop decay, parton shower and hadronisation: in fact, as shown in [23], the possibility of extracting such effects is generally limited by systematics rather than statistics.

Acknowledgments

We thank Claudio Verzegnassi for discussions and for financial support during a visit to Trieste. SM also acknowledges useful conversations and email exchanges with Matteo Beccaria,

References

- [1] E. Maina and S. Moretti, Phys. Lett. B **286** (1992) 370.
- [2] P. Uwer, Phys. Lett. B **609** (2005) 271; W. Bernreuther, A. Brandenburg, Z.G. Si and P. Uwer, arXiv:hep-ph/0410197, Nucl. Phys. B **690** (2004) 81, Acta Phys. Polon. B **34** (2003) 4477, arXiv:hep-ph/0209202, Int. J. Mod. Phys. A **18** (2003) 1357, Phys. Rev. Lett. **87** (2001) 242002, Phys. Lett. B **509** (2001) 53; A. Brandenburg, Z.G. Si and P. Uwer, Phys. Lett. B **539** (2002) 235; W. Bernreuther, A. Brandenburg and P. Uwer, Phys. Lett. B **368** (1996) 153.
- [3] W. Wagner, Rept. Prog. Phys. **68** (2005) 2409.
- [4] M. Beccaria, S. Bentvelsen, M. Cöbalt, F.M. Renard and C. Verzegnassi, Phys. Rev. D **71** (2005) 073003.
- [5] P. Nason, S. Dawson and R.K. Ellis, Nucl. Phys. B **303** (1988) 607 and Nucl. Phys. B **327** (1989) 49; W. Beenakker, H. Kuijf, W.L. van Neerven and J. Smith, Phys. Rev. D **40** (1989) 54; W. Beenakker, W.L. van Neerven, R. Meng, G.A. Schuler and J. Smith, Nucl. Phys. B **351** (1991) 507; M.L. Mangano, P. Nason and G. Ridolfi, Nucl. Phys. B **373** (1992) 295.
- [6] J.H. Kuhn, A. Scharf and P. Uwer, Eur. Phys. J. C **45** (2006) 139.
- [7] W. Bernreuther, M. Fickler and Z.G. Si, Phys. Lett. B **633** (2006) 54, arXiv:hep-ph/0509210.
- [8] W. Beenakker, A. Denner, W. Hollik, R. Mertig, T. Sack and D. Wackeroth, Nucl. Phys. B **411** (1994) 343; C. Kao, G.A. Ladinsky and C.P. Yuan, Int. J. Mod. Phys. A **12** (1997) 1341; C. Kao and Doreen Wackeroth, Phys. Rev. D **61** (2000) 055009.
- [9] L.D. Landau, Dokl. Akad. Nauk SSSR **60** (1948) 207; C.N. Yang, Phys. Rev. **77** (1950) 242.
- [10] M. Melles, Phys. Rept. **375** (2003) 219.
- [11] A. Denner, arXiv:hep-ph/0110155; A. Denner and S. Pozzorini, Eur. Phys. J. C **18** (2001) 461 and Eur. Phys. J. C **21** (2001) 63.
- [12] M. Ciafaloni, P. Ciafaloni and D. Comelli, Phys. Rev. Lett. **84** (2000) 4810, Nucl. Phys. B **589** (2000) 359.
- [13] J.A.M. Vermaseren, arXiv:math-ph/0010025.

- [14] J. Kublbeck, M. Bohm and A. Denner, *Comput. Phys. Commun.* **60** (1990) 165.
- [15] M. Beccaria, F.M. Renard and C. Verzegnassi, *Phys. Rev. D* **69** (2004) 113004 and arXiv:hep-ph/0405036.
- [16] M. Beccaria, F.M. Renard and C. Verzegnassi, *Phys. Rev. D* **72** (2005) 093001.
- [17] J. Pumplin, D.R. Stump, J. Huston, H.L. Lai, P. Nadolsky and W.-K. Tung, *JHEP* **0207** (2002) 012.
- [18] E. Maina, S. Moretti, M.R. Nolten and D.A. Ross, *Phys. Lett. B* **570** (2003) 205.
- [19] S. Moretti, M.R. Nolten and D.A. Ross, arXiv:hep-ph/0503152.
- [20] J.R. Ellis, S. Moretti and D.A. Ross, *JHEP* **0106** (2001) 043.
- [21] S. Moretti, M.R. Nolten and D.A. Ross, arXiv:hep-ph/0509254.
- [22] V.S. Fadin, L.N. Lipatov, A.D. Martin and M. Melles, *Phys. Rev. D* **61** (2000) 094002; W. Beenakker and A. Werthenbach, *Nucl. Phys. B* **630** (2002) 3; A. Denner, M. Melles and S. Pozzorini, *Nucl. Phys. B* **662** (2003) 299; B. Feucht, J.H. Kuhn, A.A. Penin and V.A. Smirnov, *Phys. Rev. D* **93** (2004) 101802; B. Jantzen, J.H. Kuhn, A.A. Penin and V.A. Smirnov, *Phys. Rev. D* **72** (2005) 051301.
- [23] F. Hubaut, E. Monnier, P. Pralavorio, K. Smolek and V. Simak, *Eur. Phys. J. C* **44S2** (2005) 13.

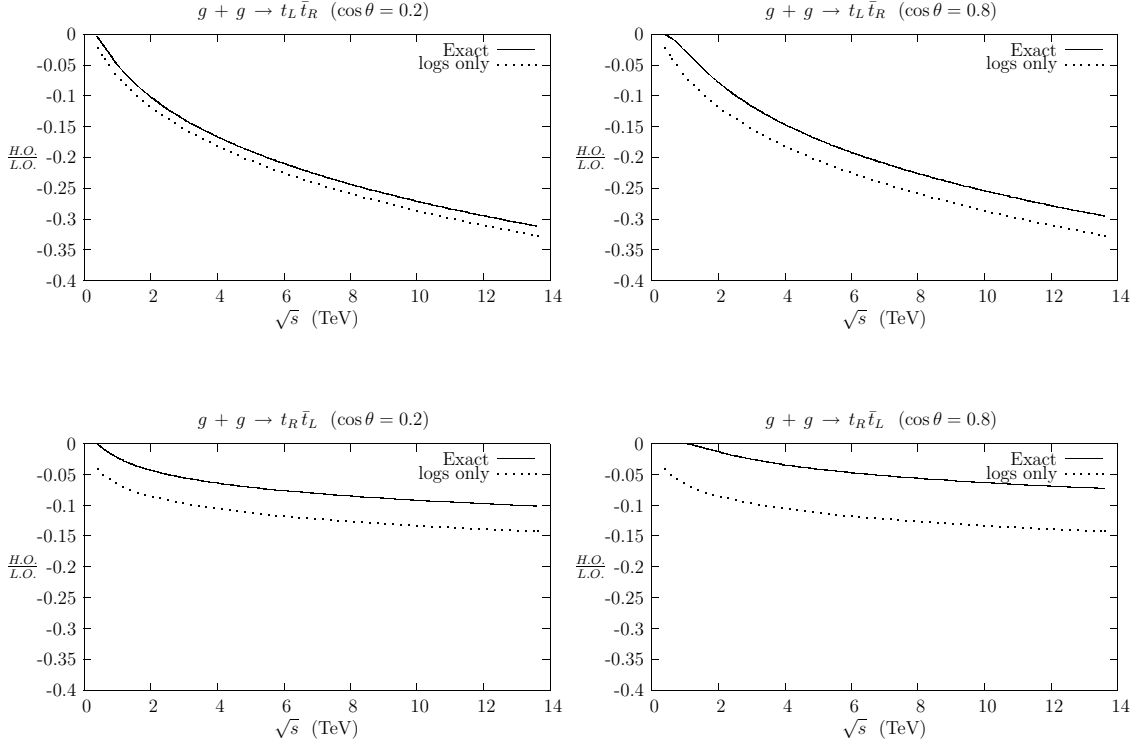


Figure 4: A comparison of the exact $\mathcal{O}(\alpha_s^2 \alpha_W)$ corrections to those obtained from angular independent (double and single) logarithms only in Ref. [4], for the two combinations with opposite helicities in the final state. The graphs on the left(right) represent the case of large(small) angle scattering. Notice that we have subtracted the EM contributions from the formulae in Ref. [4].

Weak corrections to gluon-induced top-antitop hadro-production: Erratum

S. Moretti, M.R. Nolten and D.A. Ross

School of Physics & Astronomy, University of Southampton, Southampton SO17 1BJ, UK

Abstract

This is an Erratum to a paper of ours, Phys. Lett. B **639** (2006) 513. After its publication, we have discovered a mistake in a numerical program that affects the results presented therein. We provide here the corrected version.

New numerical results

The numerical program used to produce the results of Ref. [1] was affected by a mistake, which has now been corrected. We present in Figs. 1–3 the amended results, in correspondence to the same figures in the original paper. We also note, as remarked in [2], that the parity-violating asymmetry A_{PV} defined in [1] is identically zero through $\mathcal{O}(\alpha_S^2\alpha_W)$, as we could now verify explicitly. The inclusive results are now as follow: while the (Higgs mass independent) tree-level cross section for $gg \rightarrow t\bar{t}$ at the LHC is 384 pb, we now find that the weak corrections through $\mathcal{O}(\alpha_S^2\alpha_W)$ amount to -9.65 pb for $M_H = 150$ GeV and -9.39 pb for $M_H = 200$ GeV. All these plots and cross sections correspond to the numerical setup (masses, couplings, PDFs, scales, etc.) declared in [1].

For all such results, as well additional ones presented in Refs. [2, 3] (where independent calculations of the same corrections tackled in [1] were performed), we found very good agreement between ourselves and Refs. [2, 3], for the same choice of input parameters.

As for Fig. 4 of [1], here the differences are not substantial. Besides, the purpose of those plots was to illustrate the difference between the full results and the Sudakov approximation, which is largely unaffected by the correction we made to our program. Hence, we do not reproduce those plots here.

Finally, we have now also calculated the $\mathcal{O}(\alpha_S^2\alpha_W)$ corrections to the $q\bar{q} \rightarrow t\bar{t}$ subprocess and the results obtained (not shown here) are in agreement with the corresponding ones in Refs. [4, 5].

Acknowledgments

We are extremely grateful to Werner Bernreuther, Michael Fückers and Peter Uwer for their help in checking our program and finding the source of the discrepancies between our results and theirs.

References

- [1] S. Moretti, M.R. Nolten and D.A. Ross, Phys. Lett. B **639** (2006) 513.
- [2] W. Bernreuther, M. Fückers and Z. G. Si, Phys. Rev. D **74** (2006) 113005.
- [3] J. H. Kühn, A. Scharf and P. Uwer, Eur. Phys. J. C **51** (2007) 37.
- [4] W. Bernreuther, M. Fückers and Z. G. Si, Phys. Lett. B **633** (2006) 54.
- [5] J. H. Kühn, A. Scharf and P. Uwer, Eur. Phys. J. C **45** (2006) 139.

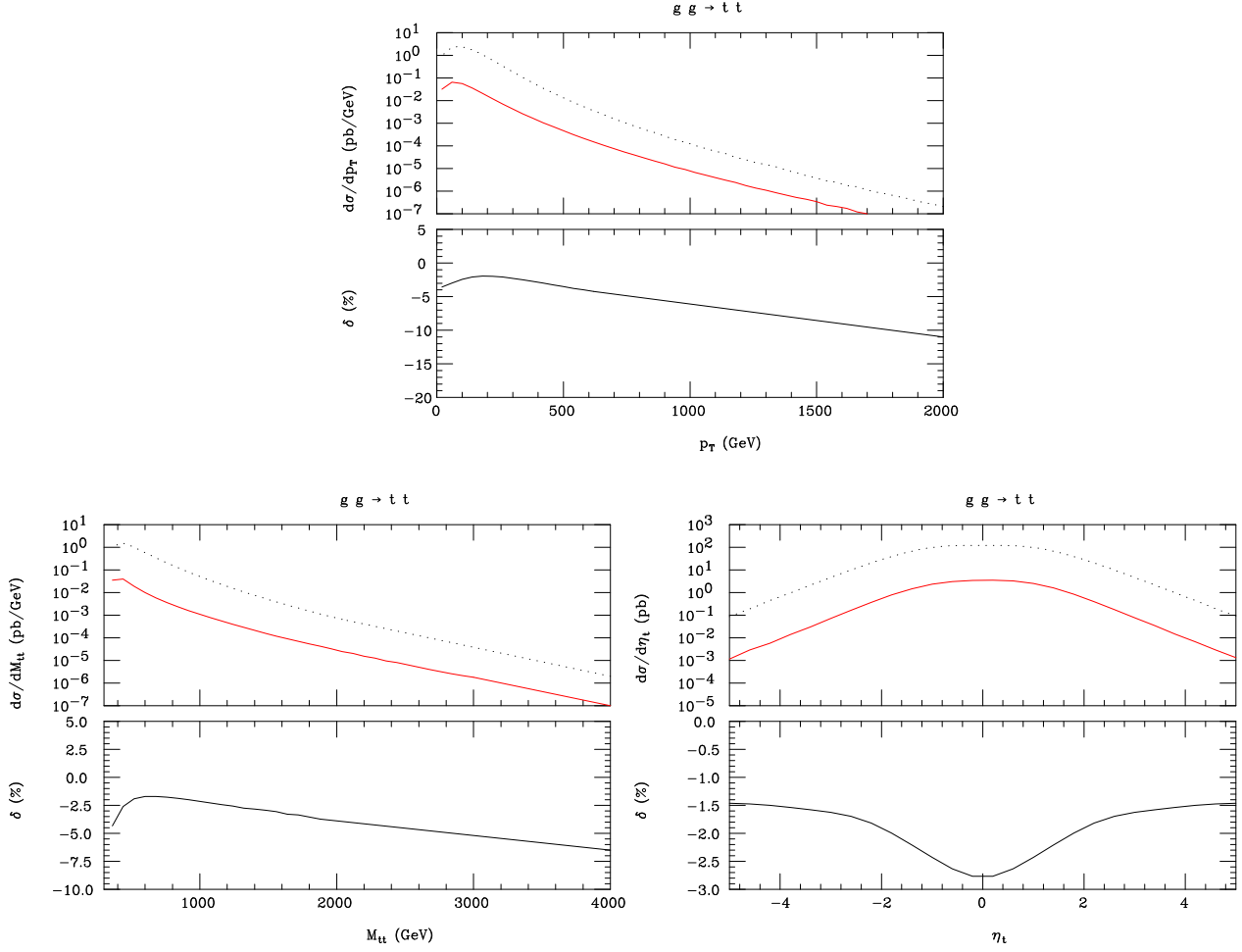


Figure 5: Differential distributions of the subprocess $gg \rightarrow t\bar{t}$ through the $\mathcal{O}(\alpha_s^2)$ (top frames, dotted) and the $\mathcal{O}(\alpha_s^2 \alpha_W)$ (top frames, solid) as well as the percentage of the latter with respect to the former (bottom frames, solid) for the (anti)top transverse momentum p_T , the top-antitop invariant mass $M_{t\bar{t}}$ and the (anti)top pseudorapidity η_t . (Lightly/Red coloured solid tracts in logarithmic scale are intended to be negative.)

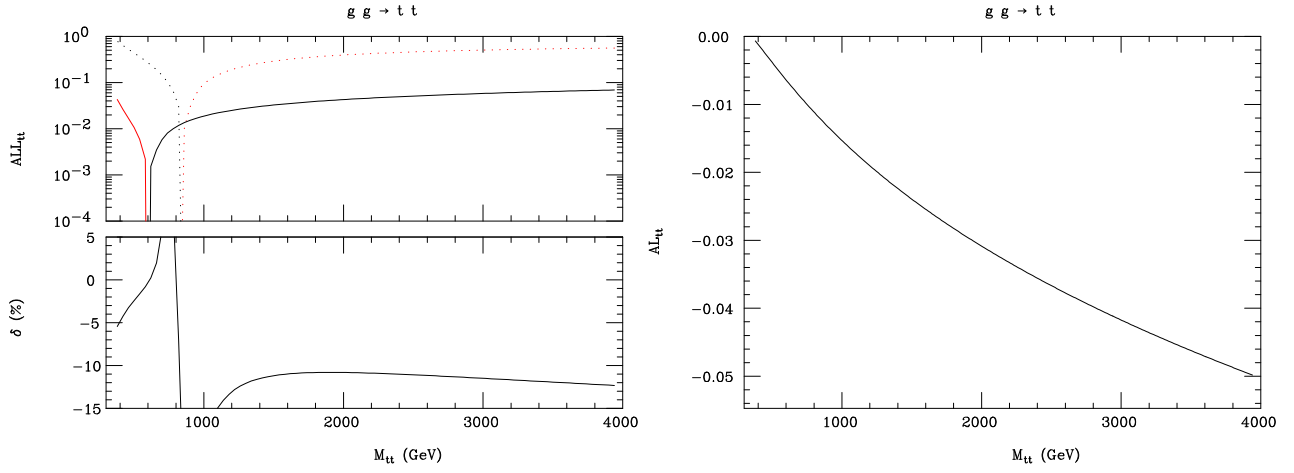


Figure 6: The differential spin asymmetry A_{LL} (as defined in [1]) of the subprocess $gg \rightarrow t\bar{t}$ through the $\mathcal{O}(\alpha_S^2)$ (left plot, top frame, dotted) and the $\mathcal{O}(\alpha_S^2\alpha_W)$ (left plot, top frame, solid). (Note that the LO QCD contribution changes sign at ≈ 900 GeV and is heavily dependent on $M_{t\bar{t}}$ whereas the $\mathcal{O}(\alpha_S^2\alpha_W)$ correction is not.) In the left plot, bottom frame, we show the percentage correction to the (non-zero) LO QCD asymmetry for A_{LL} due to $\mathcal{O}(\alpha_S^2\alpha_W)$ effects. The right plot displays the asymmetry A_L (as defined in [1]), which vanishes exactly in LO QCD, through the same order. The asymmetries are calculated along the helicity axis as a function of the top-antitop invariant mass $M_{t\bar{t}}$.

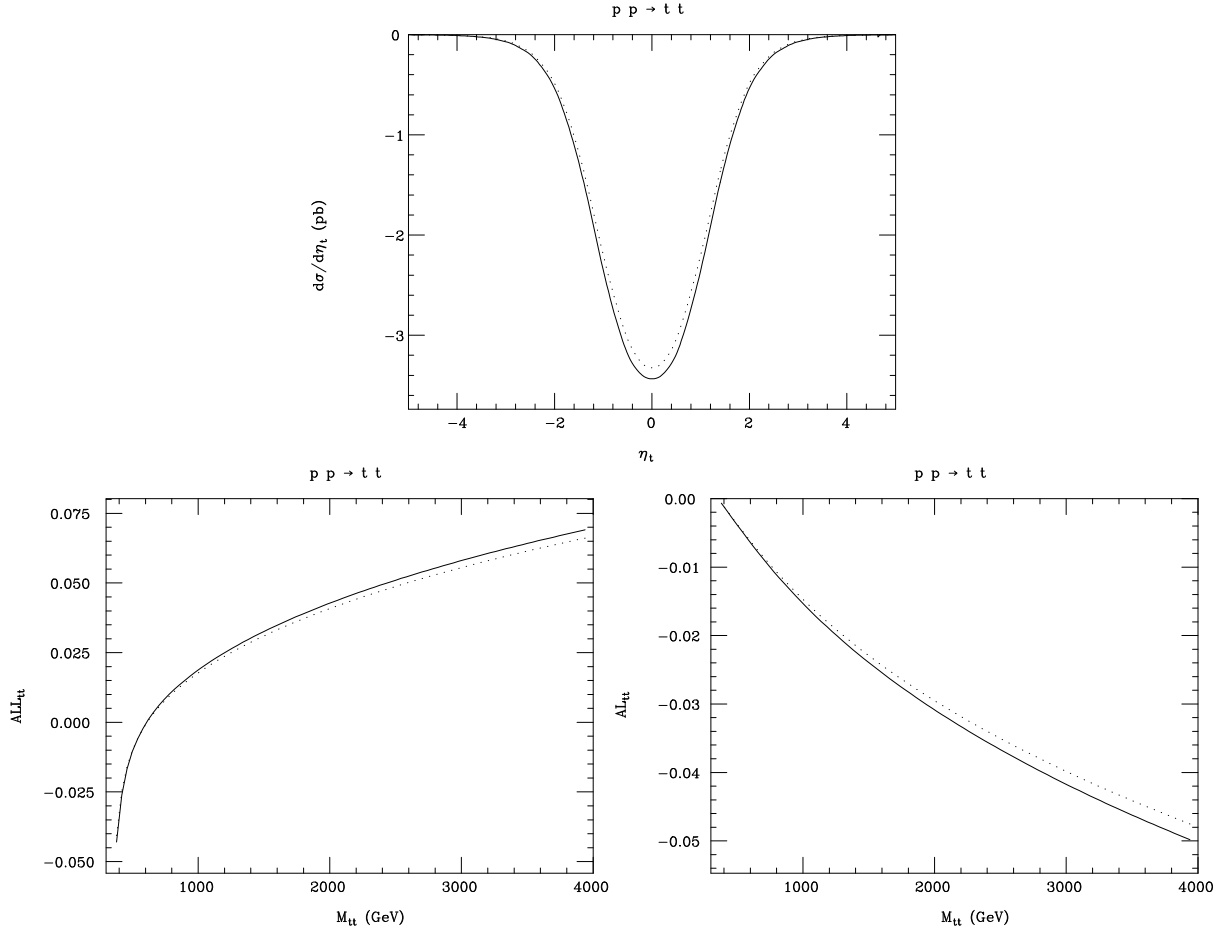


Figure 7: The absolute size of the $\mathcal{O}(\alpha_s^2 \alpha_W)$ corrections to the subprocess $gg \rightarrow t\bar{t}$ for the distribution in (anti)top pseudorapidity η_t (top plot) and the differential spin asymmetries (bottom plots, as defined in [1]), for $M_H = 150$ GeV (solid) and $M_H = 200$ GeV (dotted). The asymmetries are calculated along the helicity axis as a function of the top-antitop invariant mass $M_{t\bar{t}}$.